Supporting Information

Ultrathin lithium aluminate nanoflakes inlaid sulfur as cathode material for lithium–sulfur batteries with high areal capacity

Arnab Ghosh,[1,2,3] Ajit Kumar,[1,2,3] Amlan Roy,[3] Cuong Nguyen,[2] Aakash Ahuja,[3] Md. Adil,[3] Manjunath Chatti,[2] Mega Kar,[2,*] Douglas R. MacFarlane,[2,*] and Sagar Mitra[3,*]

[1]IITB-Monash Research Academy, Powai, Mumbai 400076, India.

[2]ARC Centre of Excellence for Electromaterials Science, School of Chemistry, Monash University, Clayton, Victoria 3800, Australia.

[3]Electrochemical Energy Laboratory, Department of Energy Science and Engineering, Indian Institute of Technology Bombay, Mumbai 400076, India.

Corresponding authors

*E-mail: mega.kar@monash.edu

*E-mail: douglas.macfarlane@monash.edu

*E-mail: sagar.mitra@iitb.ac.in

List of supporting contents

Elemental mapping of $LiAlO_2$

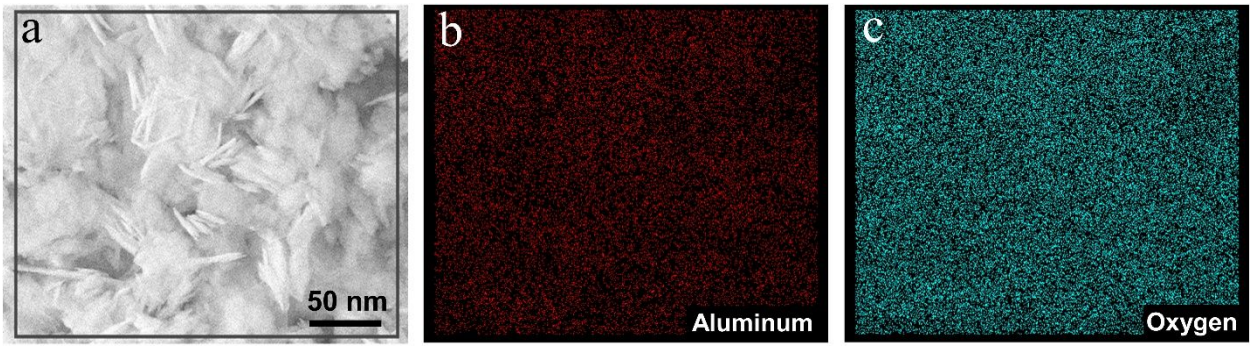

Figure S1: (a–c) SEM image and elemental mapping of $LiAlO_2$ nanoflakes.

XRD pattern of $LiAlO_2$

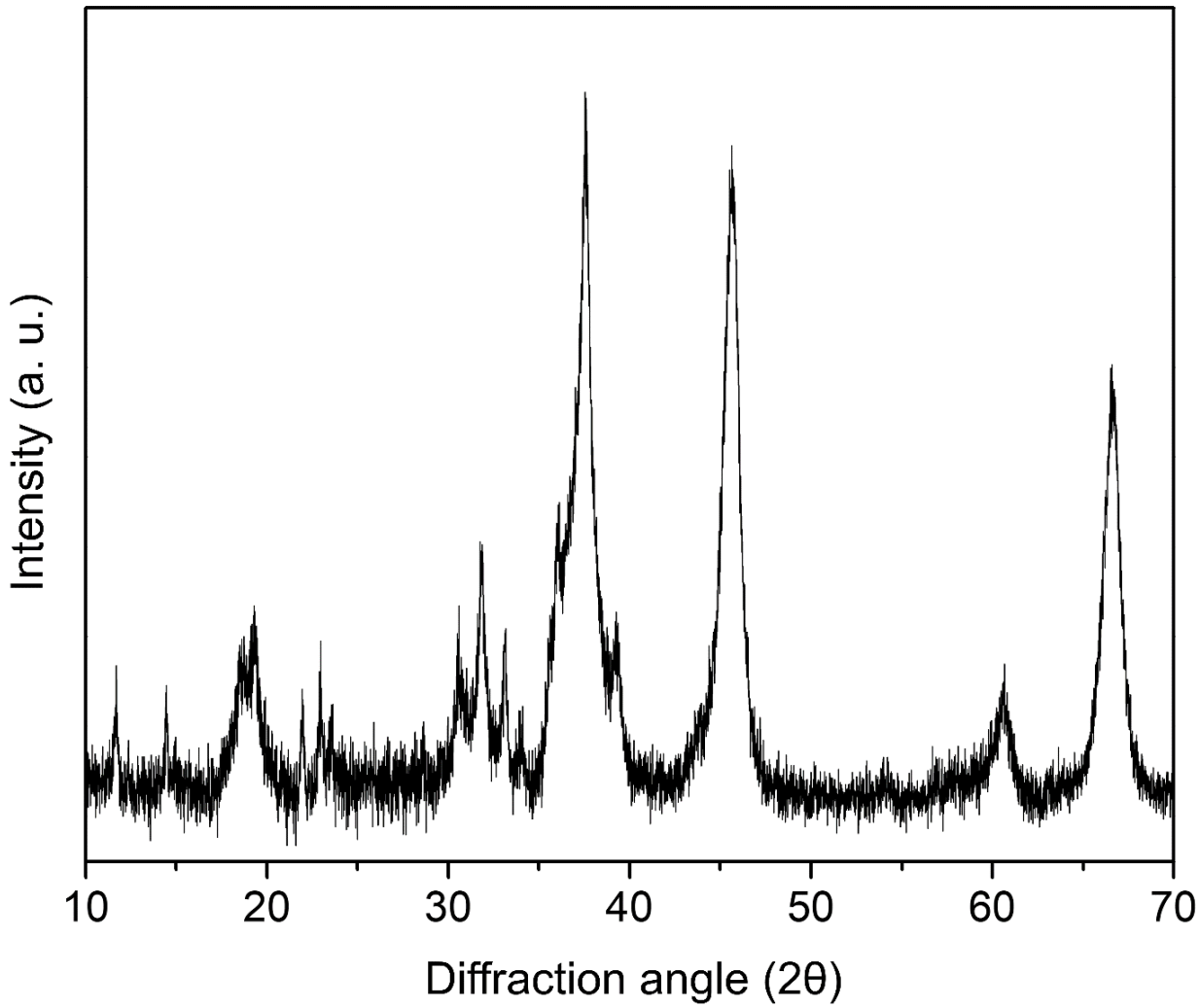

Figure S2: X-ray diffraction pattern of ultrathin α-$LiAlO_2$ nanoflakes.

Elemental mapping on S@$LiAlO_2$

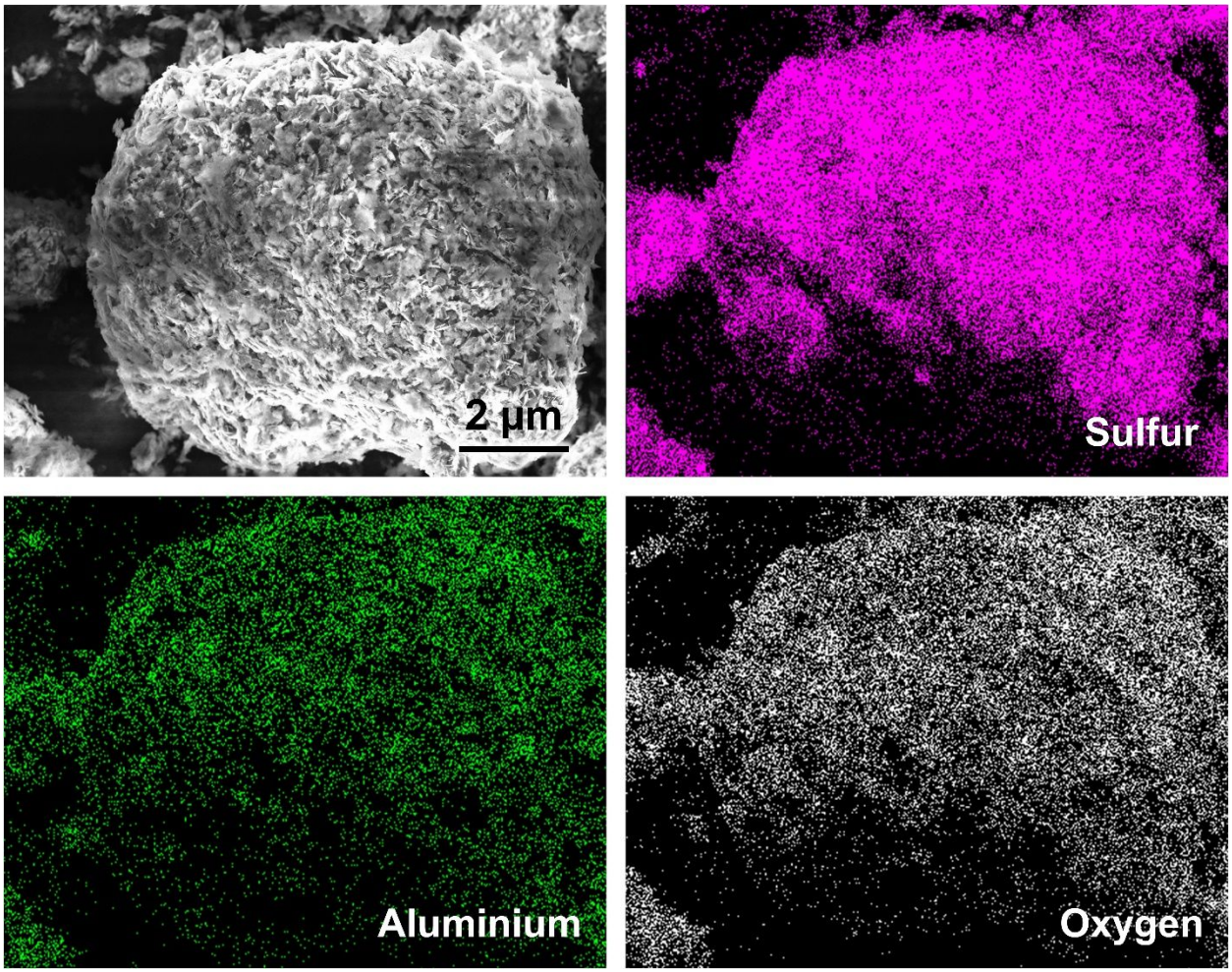

Figure S3: Elemental mapping recorded on a S@$LiAlO_2$ composite particle shows a uniform distribution of constituent elements: sulfur, aluminium and oxygen.

TEM image of S@$LiAlO_2$

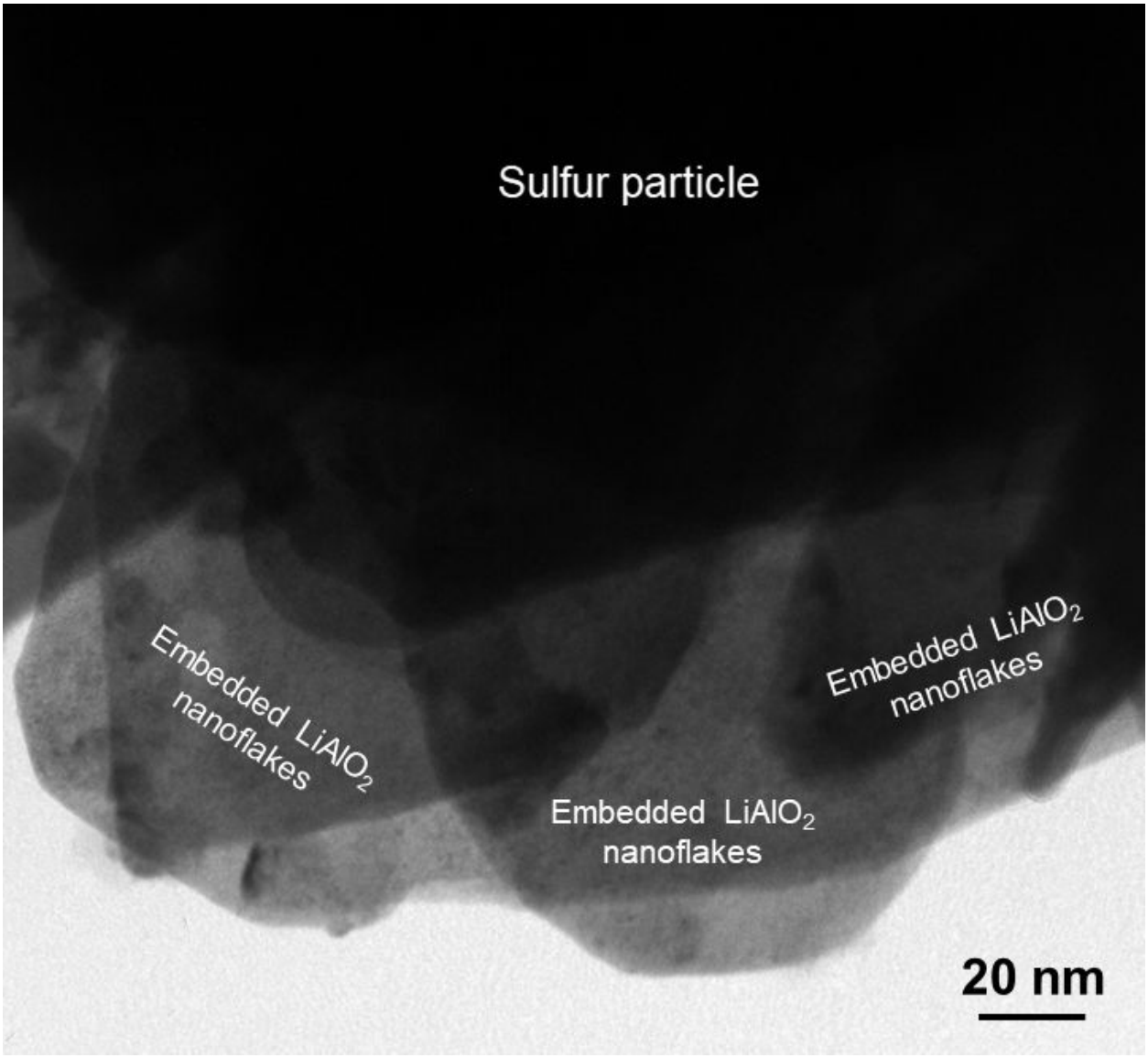

Figure S4: TEM image of S@$LiAlO_2$ composite shows $LiAlO_2$ nanoflakes are strongly adhered on the surface of the sulfur microparticles.

XRD patterns of elemental sulfur, $LiAlO_2$ and S@$LiAlO_2$

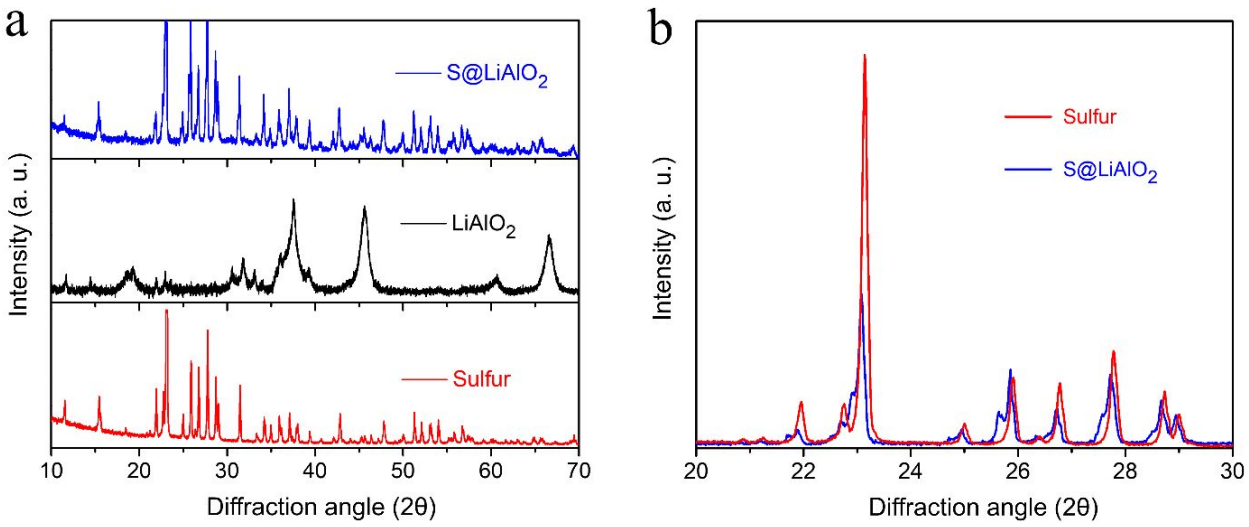

Figure S5: (a) X-ray diffraction patterns of elemental sulfur, ultrathin α-$LiAlO_2$ nanoflakes and S@$LiAlO_2$ composite, (b) merged XRD pattern of sulfur and S@$LiAlO_2$ composite.

TGA profile of $S@LiAlO_2$

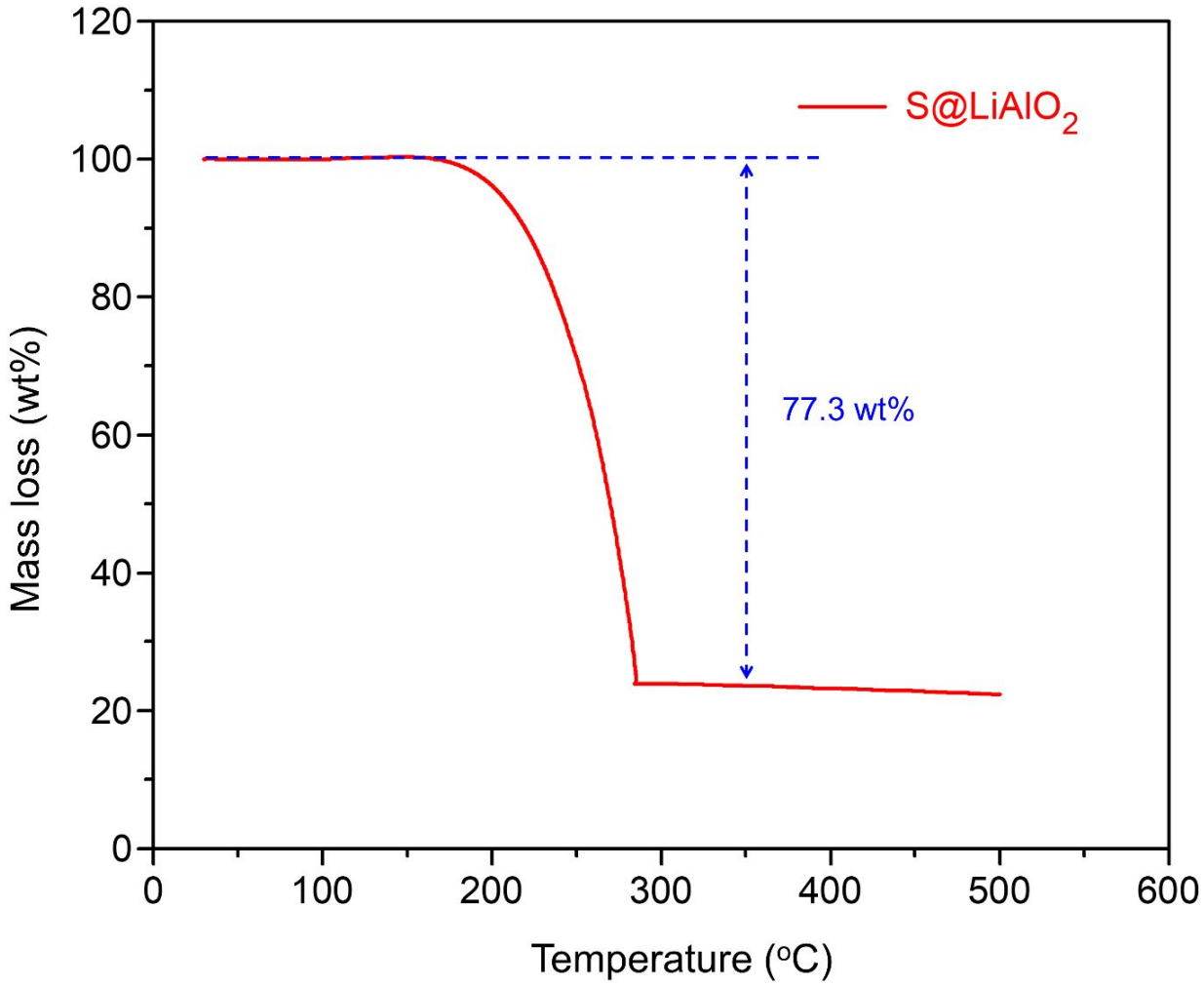

Figure S6: TGA profile of $S@LiAlO_2$ composite confirms the presence of 77.3 wt% sulfur.

Discharge profiles of S@$LiAlO_2$ cathode

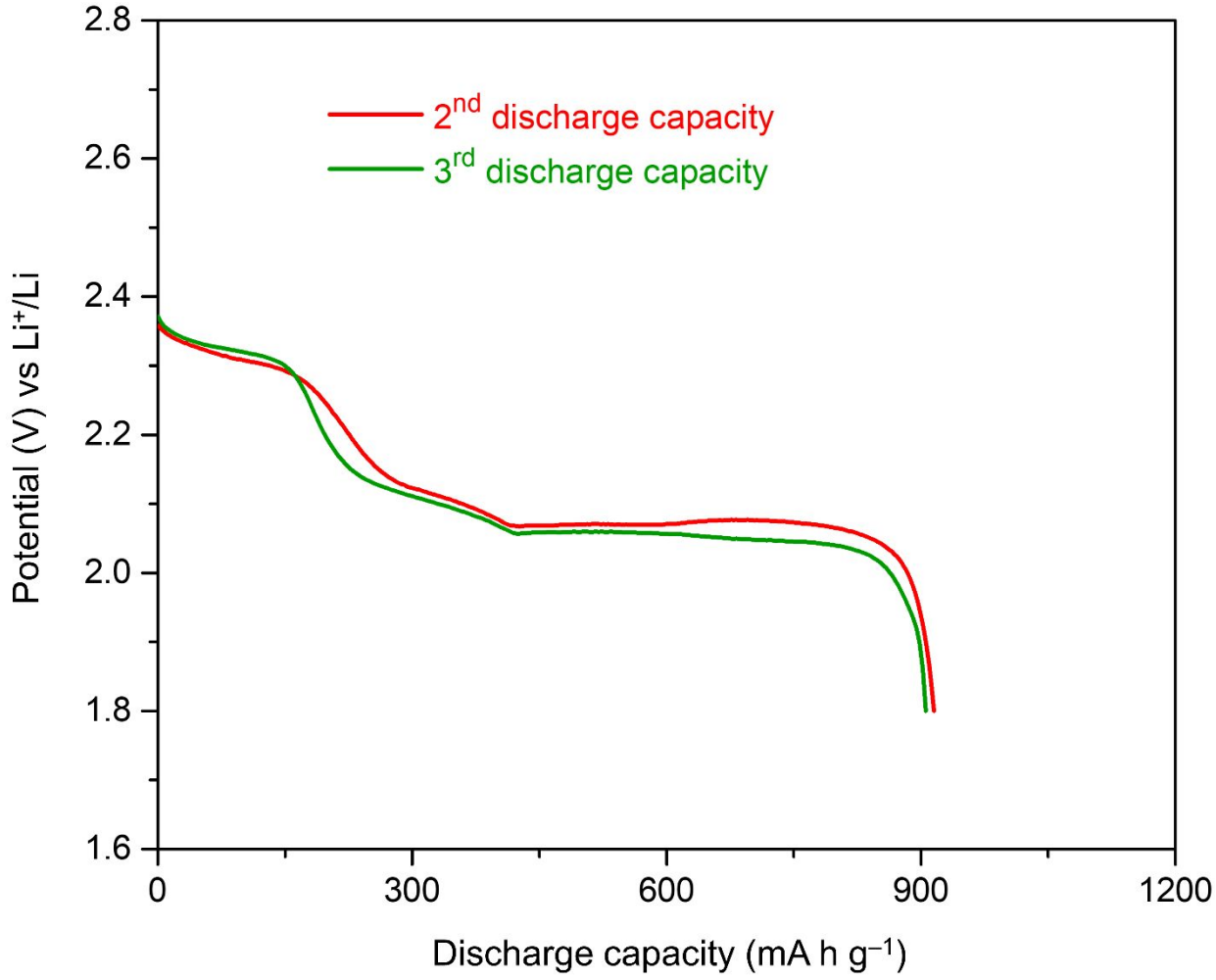

Figure S7: Second and third cycle discharge profiles of the S@$LiAlO_2$ cathode at 0.2 C.

Calculation of average cell potential

For multistep reactions, where a cell exhibits more than one discharge plateaus, following equation is used to calculate the average potential[1]

$$Vavg = \frac{1}{\int_{Q1}^{Q2} dQ} \int_{Q1}^{Q2} VdQ$$

Where, $\int_{Q1}^{Q2} dQ$ represents the specific discharge capacity, and $\int_{Q1}^{Q2} VdQ$ (i.e., area under the curve) represents the corresponding specific discharge energy (w.r.t. the weight of sulfur).

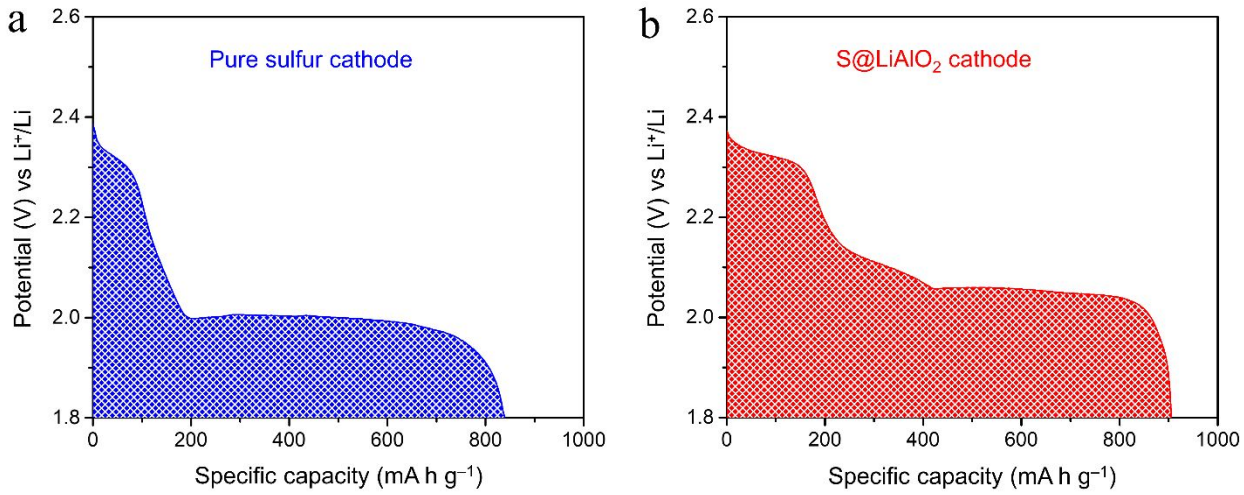

Figure S8: Second cycle discharge profile of (a) the S@CB cathode and (b) the S@$LiAlO_2$ cathode at 0.2 C current rate.

Case-1: Nominal cell potential calculation for the Li-S cell containing S@CB cathode

$\int_{Q1}^{Q2} dQ$ = specific discharge capacity of the S@CB cathode = 838.3 mA h $g_{(S)}^{-1}$

$\int_{Q1}^{Q2} VdQ$ = specific discharge energy (w.r.t. the wieght of sulfur) = 1707.7 W h $kg_{(S)}^{-1}$

Therefore, the average cell potential (V_{avg}) is estimated to be ~2.04 V.

Case-2: Nominal cell potential calculation for the Li-S cell containing S@$LiAlO_2$ cathode

$\int_{Q1}^{Q2} dQ$ = specific discharge capacity of the S@$LiAlO_2$ cathode = 907.2 mA h $g_{(S)}^{-1}$

$\int_{Q1}^{Q2} VdQ$ = specific discharge energy (w.r.t. the wieght of sulfur) = 1921.7 W h $kg_{(S)}^{-1}$

Therefore, the average cell potential (V_{avg}) is estimated to be ~2.12 V.

Performance comparison table

Sulfur hosts	Sulfur loading in electrode, mg cm^{-2} (wt%)	Initial capacity		Cycle number	Capacity loss per cycle	References
		Gravimetric capacity (per "g" of electrode)	Areal capacity (mA h cm^{-2})			
Ultrathin $LiAlO_2$ nanoflakes	5.4 (58 wt%)	393 mA h $g_{electrode}^{-1}$ @2C	3.65 mA h cm^{-2}	300	0.017%	This work
		302 mA h $g_{electrode}^{-1}$ @3C	2.80 mA h cm^{-2}	500	0.02%	
Porous VN nanobubbles	1.2 (62.5 wt%)	600 mA h $g_{electrode}^{-1}$ @2C	1.15 mA h cm^{-2}	1000	0.027%	50
MnO_2 nanosheets	1.9 (56.6 wt%)	628 mA h $g_{electrode}^{-1}$ @0.5C	2.11 mA h cm^{-2}	1500	0.028%	51
Co-Fe mixed phosphide nanocubes	1.0 (64 wt%)	552 mA h $g_{electrode}^{-1}$ @1C	0.86 mA h cm^{-2}	500	0.043%	52
TiN nanospheres	1.1 (49.7 wt%)	325 mA h $g_{electrode}^{-1}$ @2C	0.72 mA h cm^{-2}	300	0.043%	45
Ti_3C_2 nanosheets	1.8 (64.2 wt%)	679 mA h $g_{electrode}^{-1}$ @2C	1.22 mA h cm^{-2}	400	0.057%	53
Hybrid VO_2-VN nanobelts	1.7 (61.8 wt%)	624 mA h $g_{electrode}^{-1}$ @2C	1.72 mA h cm^{-2}	800	0.06%	54
Hollow Co_3S_4 nanoboxes	1.2 (56 wt%)	481 mA h $g_{electrode}^{-1}$ @2C	1.03 mA h cm^{-2}	500	0.068%	55
Co, N-dual doped CNTs/CNS/CFC	2.03 (13 wt%)	120 mA h $g_{electrode}^{-1}$ @0.5C	1.88 mA h cm^{-2}	250	0.07%	56
CoO_x nanoflowers in N-doped CNTs	1.25 (62.5 wt%)	641 mA h $g_{electrode}^{-1}$ @1C	1.28 mA h cm^{-2}	500	0.078%	57
MoS_{2-x} nanoflakes	1.5 (60 wt%)	716 mA h $g_{electrode}^{-1}$ @0.5C	1.79 mA h cm^{-2}	600	0.08%	58
Activated CNF/hollow Co_3S_4	2.5 (53 wt%)	505 mA h $g_{electrode}^{-1}$ @1C	2.38 mA h cm^{-2}	450	0.08%	59
CoOOH microsheets	1.15 (64.2 wt%)	417 mA h $g_{electrode}^{-1}$ @1C	0.75 mA h cm^{-2}	500	0.084%	60
N-doped CNT@Co-SnS_2	3.0 (52 wt%)	552 mA h $g_{electrode}^{-1}$ @0.64C	3.18 mA h cm^{-2}	300	0.16%	61

Table S1: Comparison table shows the beneficial influence of different sulfur hosts on the electrochemical performance of sulfur cathode. The electrolytes used in all of these works are comprised of LiTFSI+$LiNO_3$ in 1:1 solvent mixture of DME and DOL. The table is arranged in the ascending order of amount of capacity loss per cycle.

Spider chart

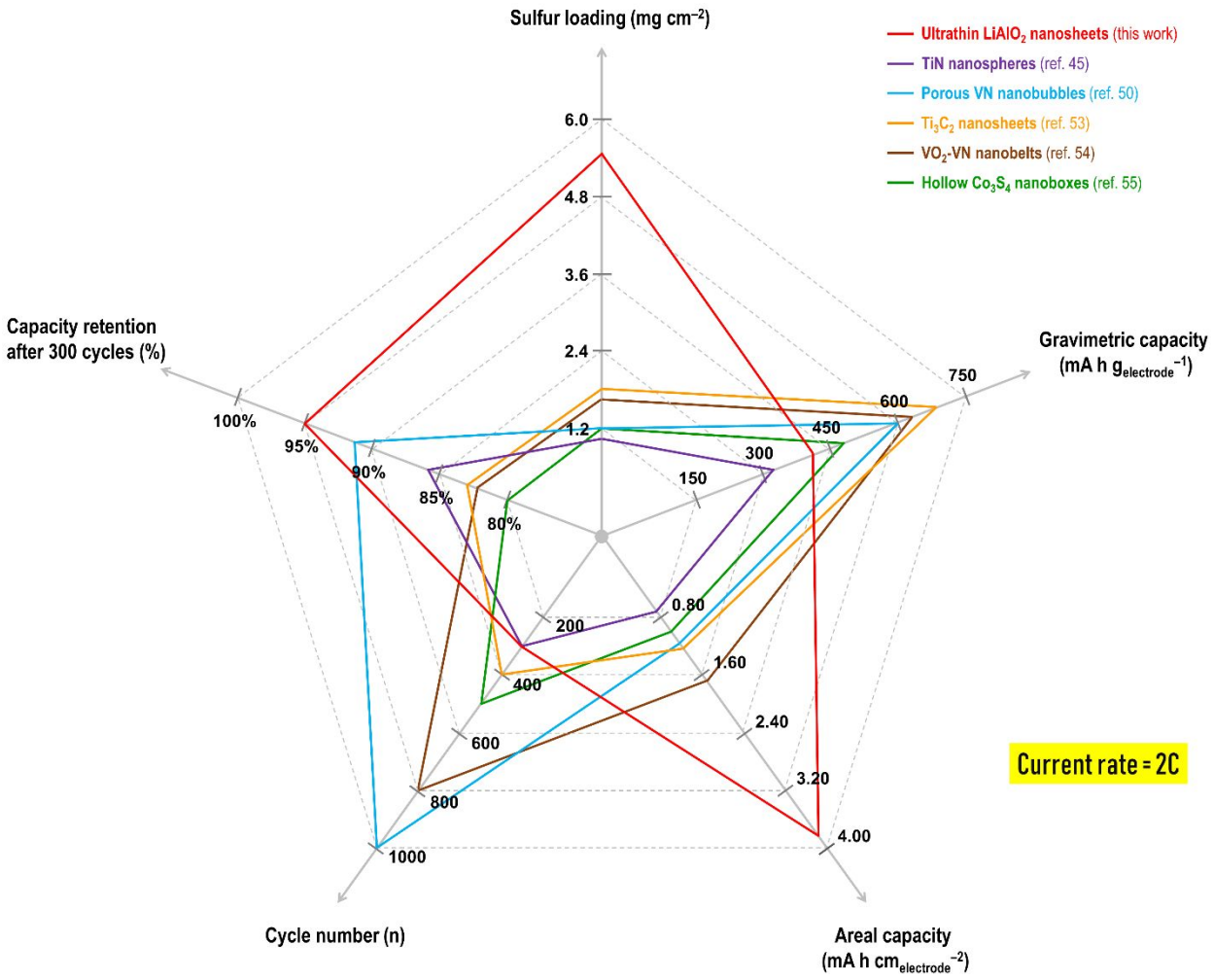

Figure S9: Spider chart compares and manifests the effective role of the ultrathin $LiAlO_2$ nanoflakes as sulfur host with other polar additives. The plot reveals the benefit of using ultrathin $LiAlO_2$ nanoflakes as an effective sulfur host in terms of promoting the higher utilization of active material (areal capacity) with unprecedented cycling stability (capacity retention after 300 cycles), even with high sulfur loading of 5.4 mg cm^{-2}. Long-term cycling performance of different cathodes at the current rate of 2C are considered for comparison.

Measurement of ionic conductivity of $LiAlO_2$

The ionic conductivity of our as-prepared α-$LiAlO_2$ was measured using a broadband dielectric spectrometer (Novocontrol Technologies, Concept 80). To measure the dc conductivity (σ_{dc}) of the sample, a pellet (diameter = 1 cm, thickness = 0.2 cm) was prepared by compressing sample at a pressure of 3.5 tons for 1 min. The as-prepared $LiAlO_2$ nanoflakes sample exhibits an ionic conductivity of 1.6 $\times 10^{-5}$ S cm^{-1} at room-temperature. The conductivity of α-$LiAlO_2$ sample was found to be enhanced with raising the temperature.

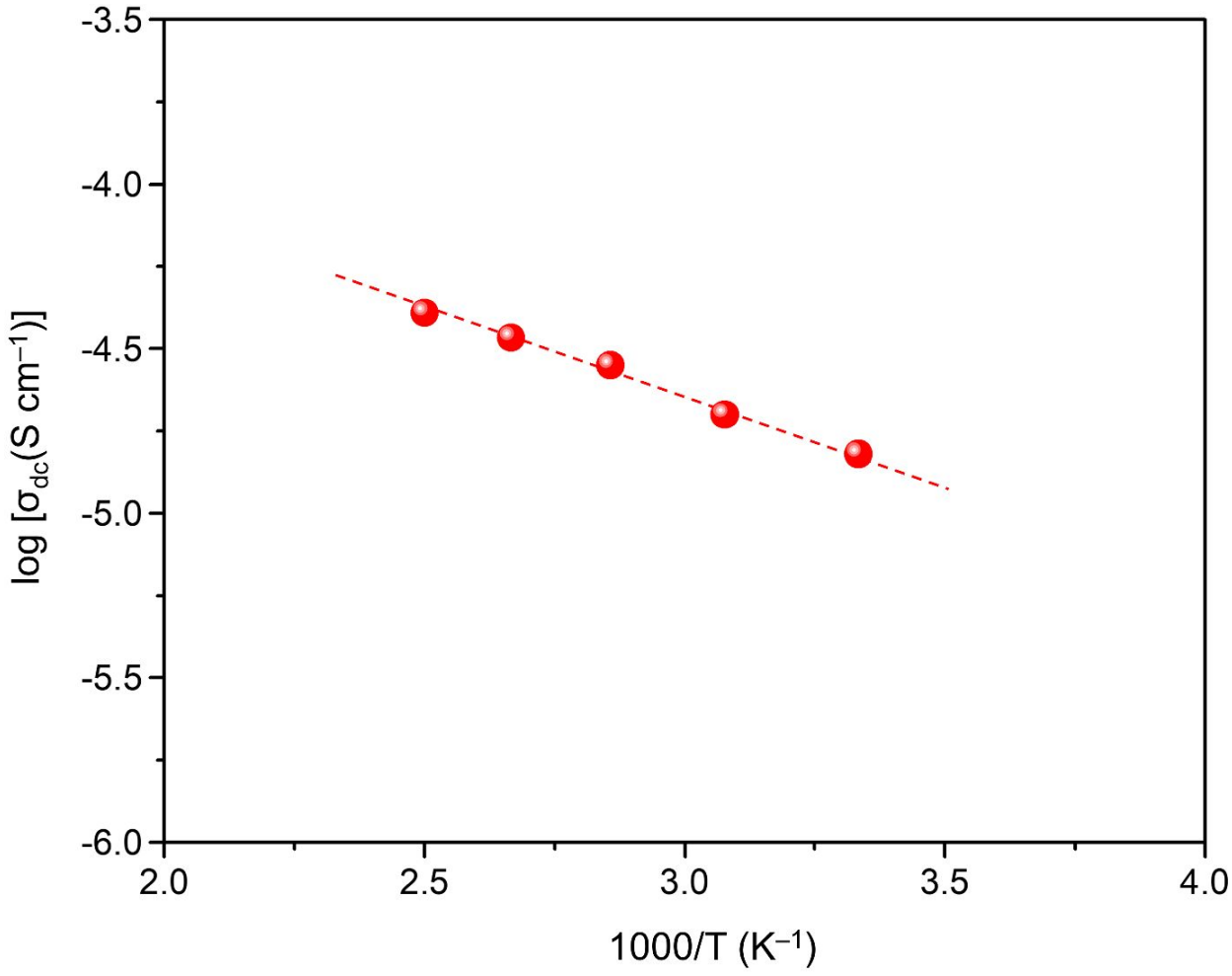

Figure S10: Arrhenius plot: change in ionic conductivity of $LiAlO_2$ nanoflakes with temperature variation.

Electrochemical impedance spectra

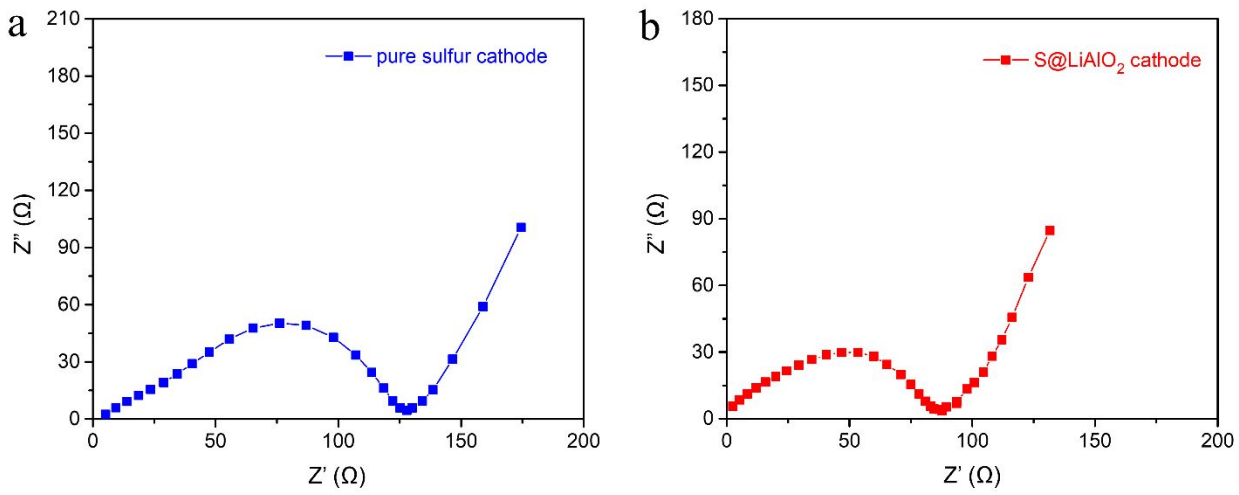

Figure S11: EIS spectra of fresh Li-S cells containing (a) S@CB cathode and (b) S@$LiAlO_2$ cathode at OCV.

Elemental mapping of S@$LiAlO_2$ loaded carbon cloth

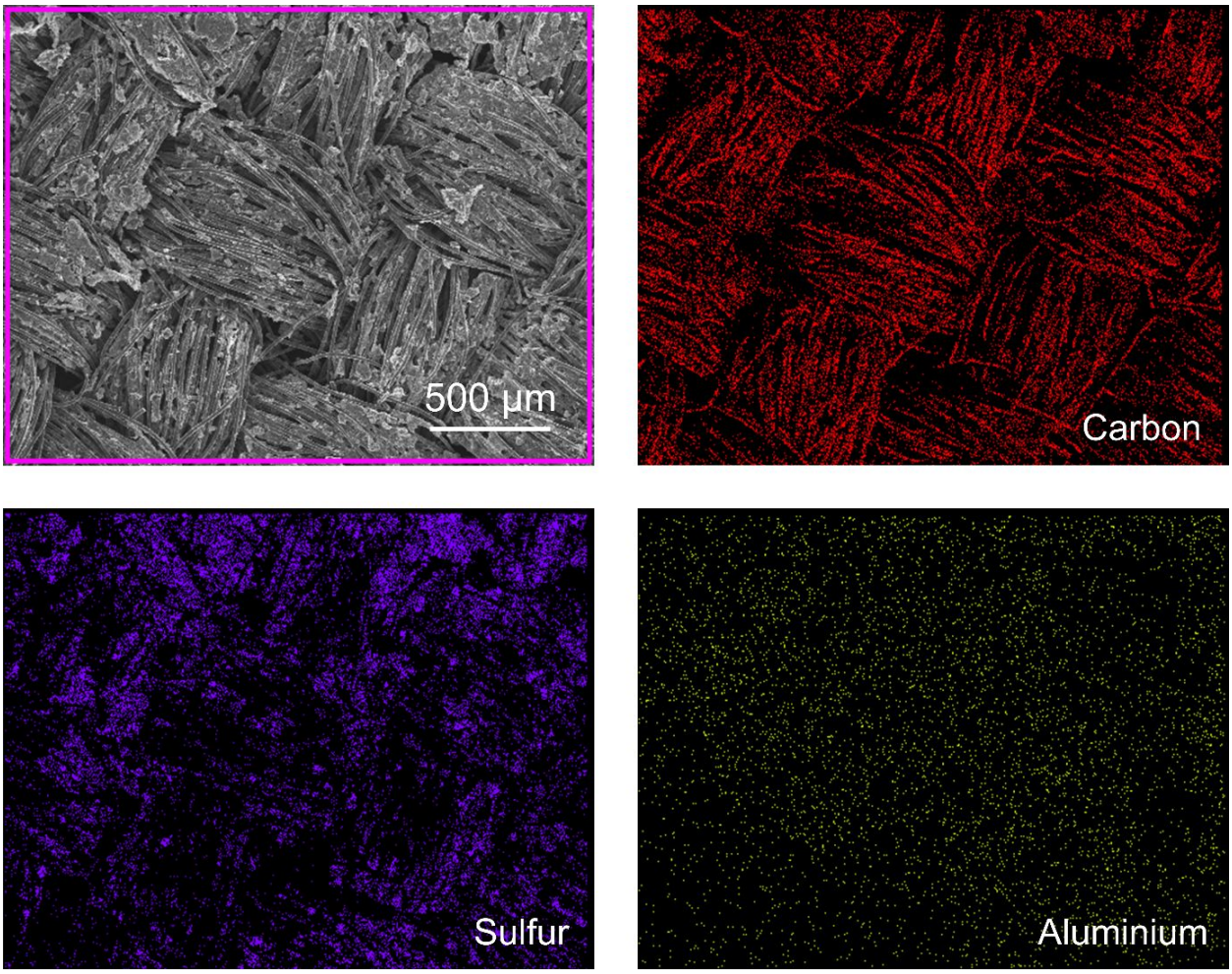

Figure S12: SEM images and elemental mapping of S@$LiAlO_2$ loaded on carbon cloth.

Polysulfide adsorption experiment

In order to confirm the polysulfide adsorption ability of ultrathin $LiAlO_2$ nanoflakes, an adsorption experiment was performed. **Figure S10a** clearly shows that after the incorporation of $LiAlO_2$ powder, the deep brown color of lithium polysulfide (Li_2S_6) solution turned colorless, indicating a strong affinity towards the polysulfides. From the UV-Vis curves the characteristic absorption peaks of the S_6^{2-} anion observed at 280, 300 and 340 nm, respectively,[2] disappeared after the incorporation of $LiAlO_2$ into the polsyulfide solution. The strong interaction between $LiAlO_2$ and Li_2S_6 is also evident from X-ray photoelectron spectroscopy (**Figure S10b**). The S $2p_{3/2}$ peak at the binding energy of 161.8 eV indicates formation of Al–S bond through Lewis acid-based interaction between the S_6^{2-} anion (Lewis base) and the positively charged Al-center in $LiAlO_2$ (Lewis acid). The SEM image shows an uniform layer of lithium polysulfide adsorbed on the surface of $LiAlO_2$ nanoflakes (**Figure S11**).

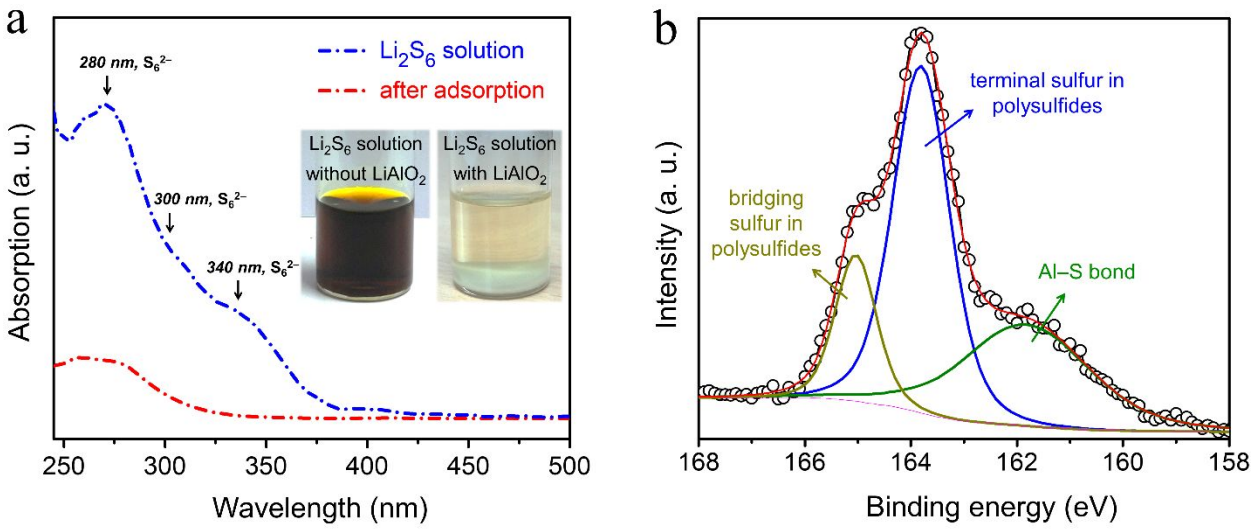

Figure S13: (a) Visualization of polysulfide adsorption by $LiAlO_2$ and corresponding UV-Vis curves; b) S $2p_{3/2}$ XPS spectra of pristine $LiAlO_2$ and polysulfide adsorbed $LiAlO_2$ samples.

SEM image of LiPS adsorbed $LiAlO_2$

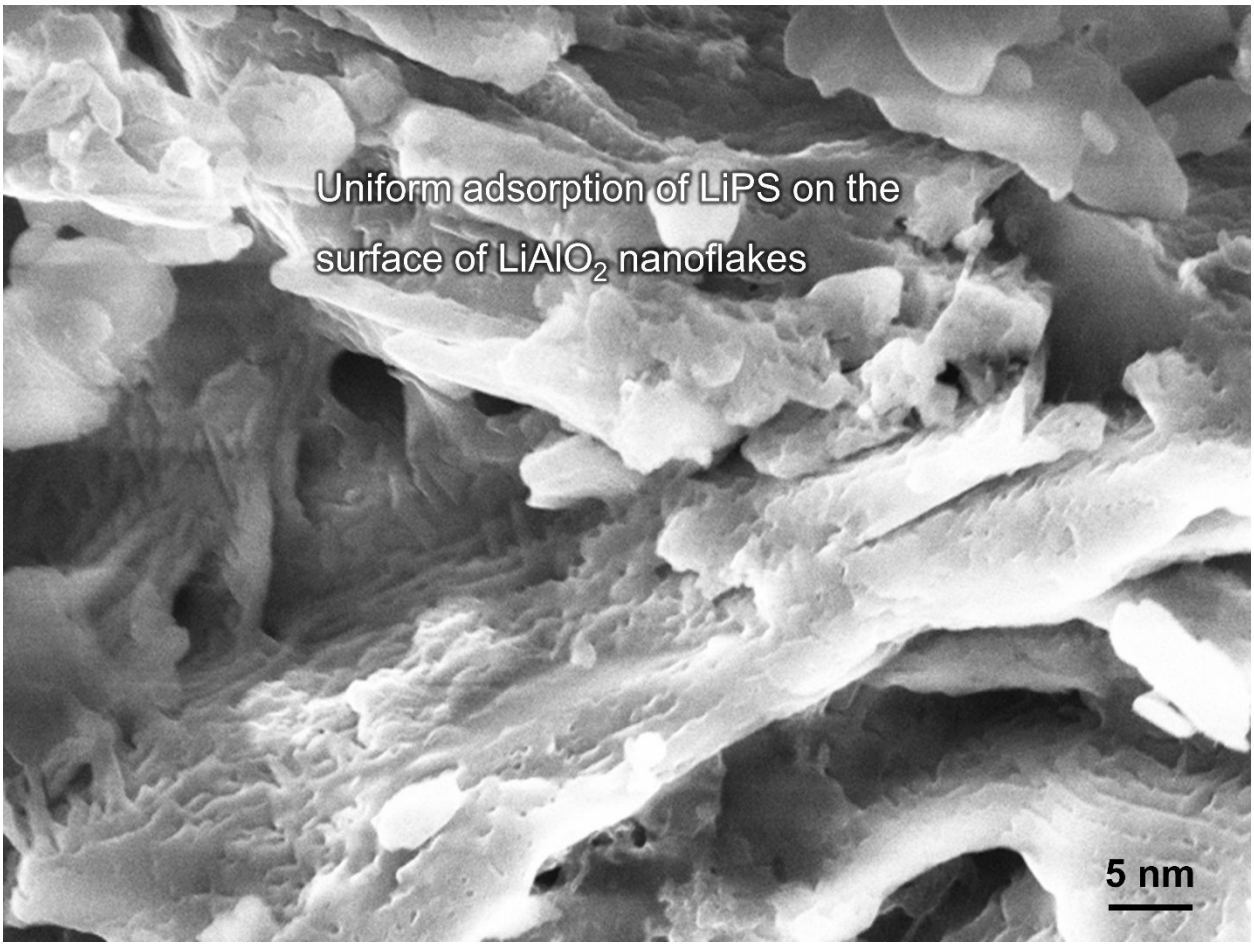

Figure S14: SEM image of polysulfide adsorbed $LiAlO_2$ nanoflakes.

Schematic of electrochemical processes in different cathodes

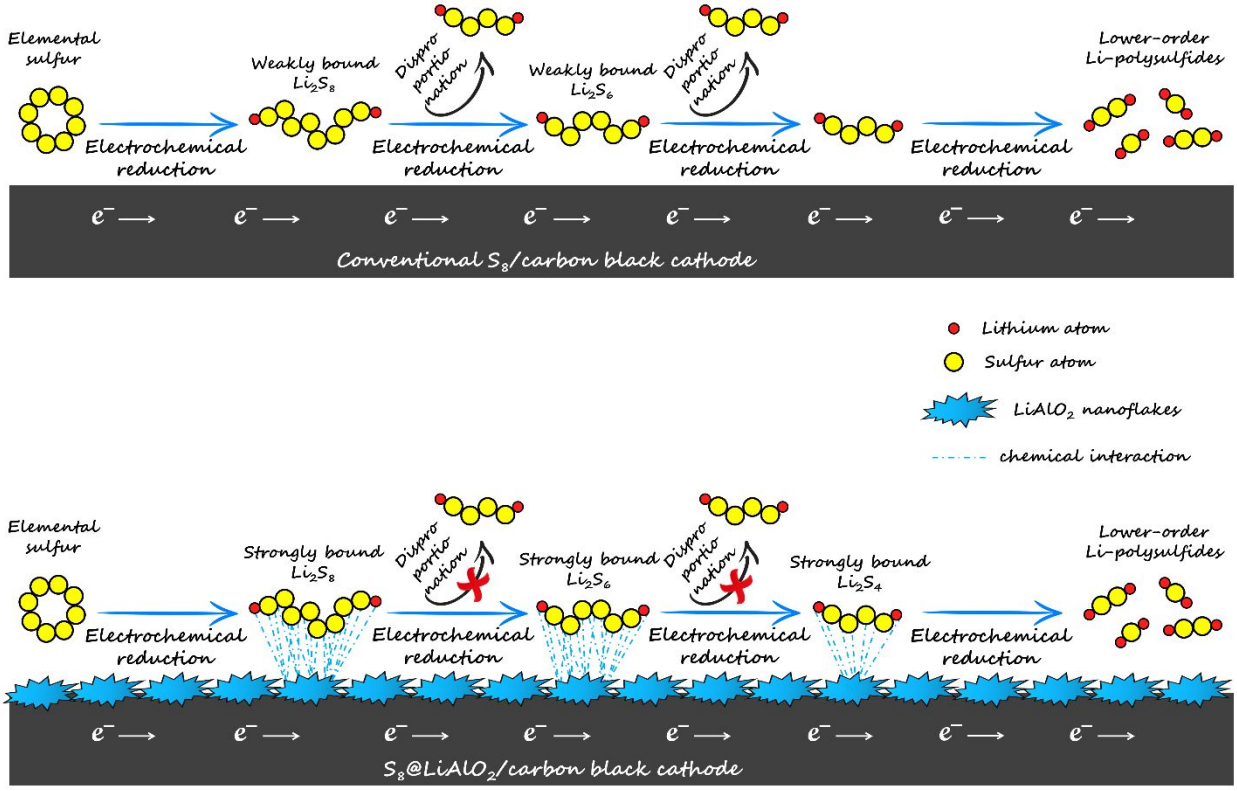

Figure S15: Schematic of different electrochemical processes in pure sulfur cathode and the S@$LiAlO_2$ cathode during discharge process.

Self-discharge study

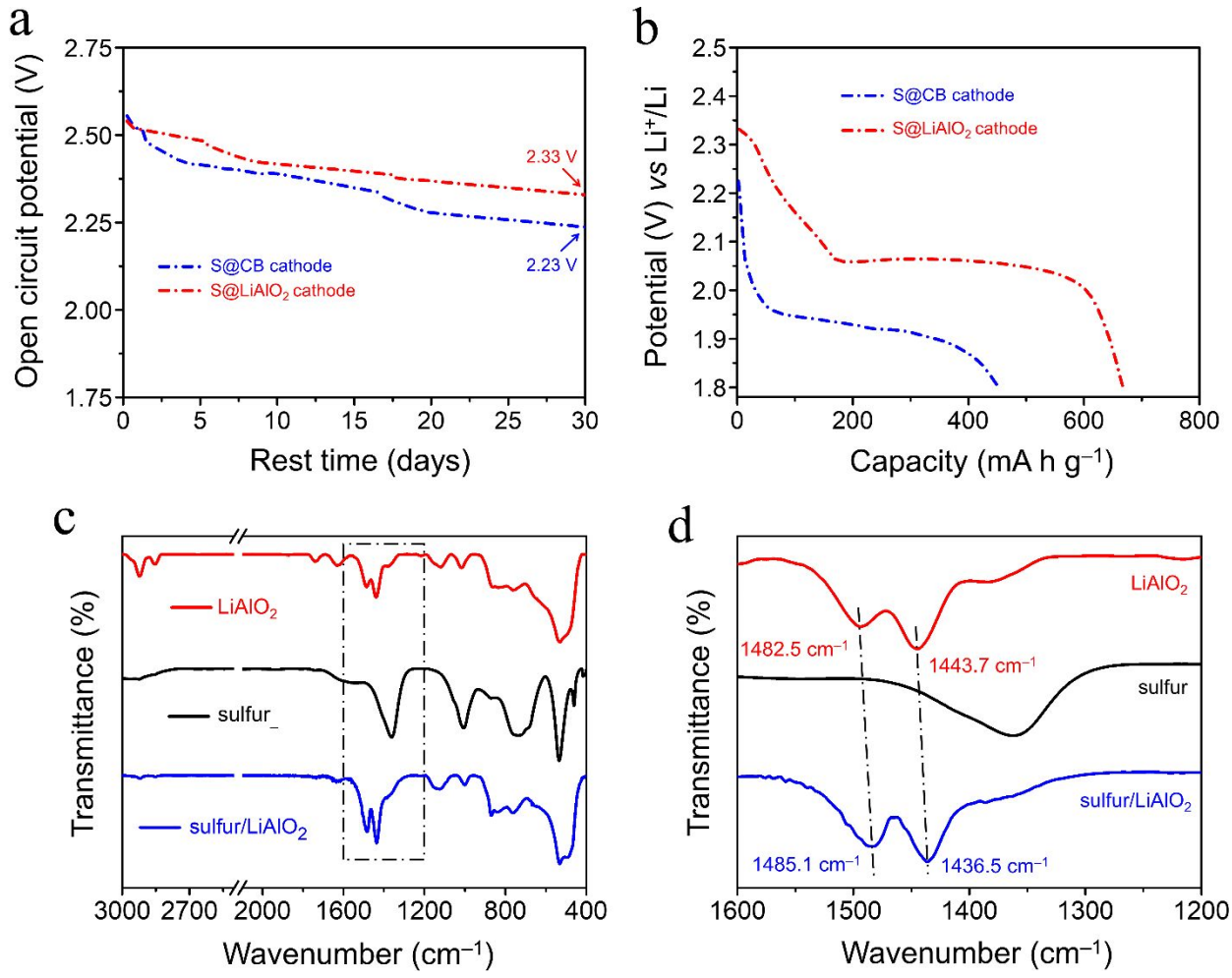

Figure S16: (a) Open-circuit voltage change of cycled cells (1 cycle at 0.2C) containing the S@CB and S@$LiAlO_2$ cathodes during resting; (b) first discharge profiles of the cells containing S@CB and S@$LiAlO_2$ cathodes after rest; (c) FTIR spectra of sulfur, $LiAlO_2$ and S@$LiAlO_2$; (d) magnified view of the spectra between 1200 cm^{-1} to 1600 cm^{-1}.

Dissolution study

Figure S17: Dissolution study of fresh S@$LiAlO_2$ cathode: the obvious no change in the color of electrolyte confirms that the uniform distribution of ultrathin $LiAlO_2$ nanoflakes on the surface of sulfur restricts the gradual dissolution of active material.

SEM image of fresh S@$LiAlO_2$ cathode

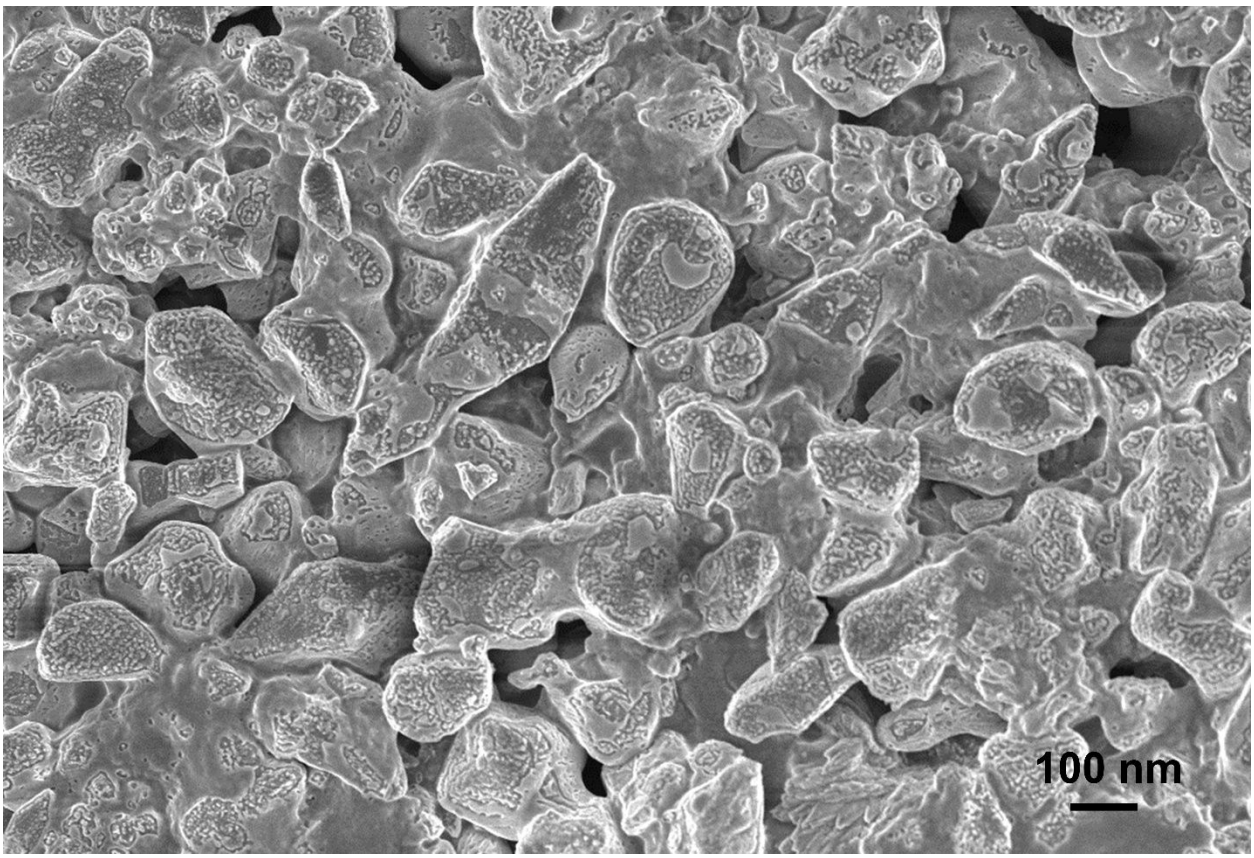

Figure S18: SEM image of fresh S@$LiAlO_2$ cathode before cycling.

SEM image of cycled S@$LiAlO_2$ cathode

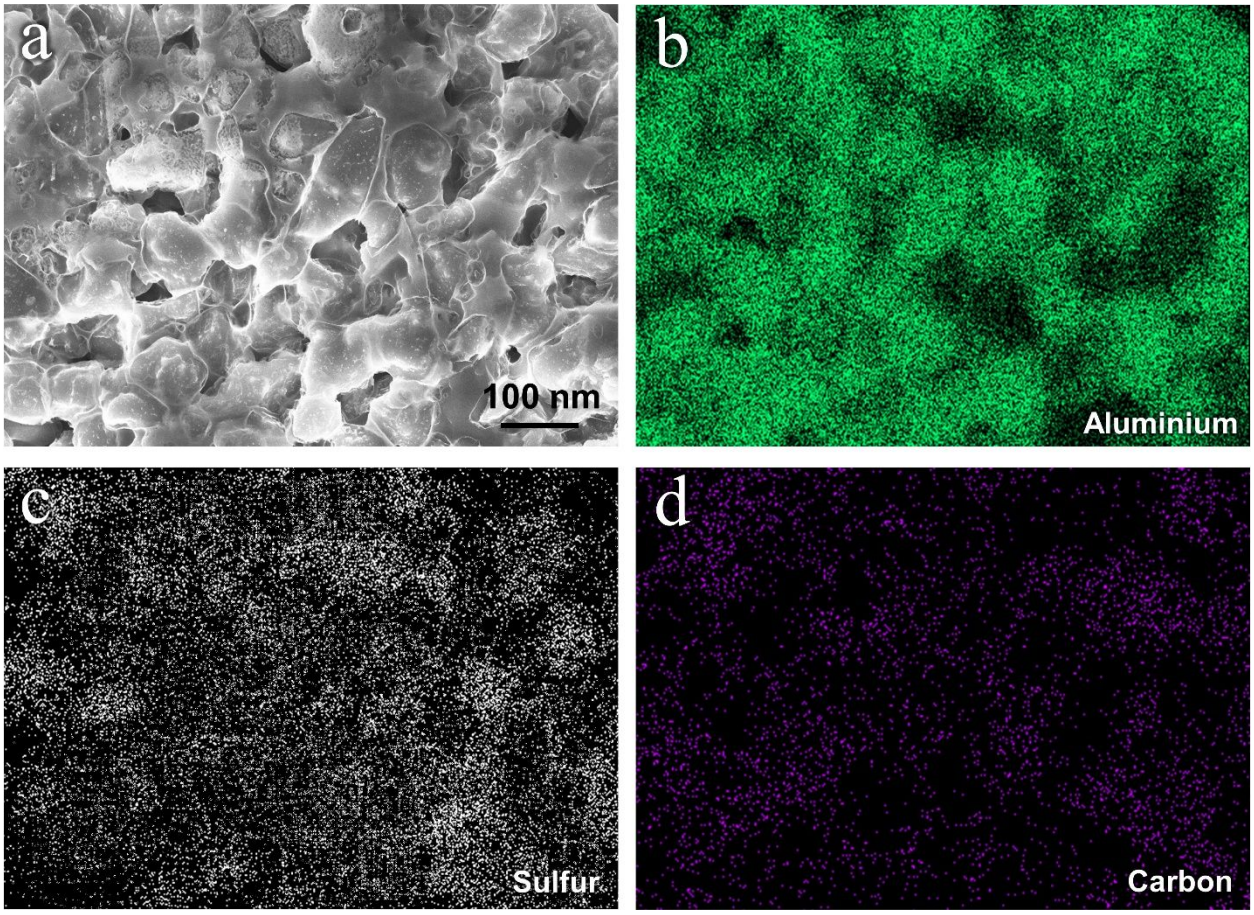

Figure S19: (a) SEM image of the cycled S@$LiAlO_2$ cathode after 300 cycles at fully charged state; (b–d) aluminium, sulfur and carbon mapping acquired on the cathode.

References

1. Xue, L.; Xin, S.; Goodenough, J. B; Angell, C. A. An Inverse Aluminum Battery: Putting the Aluminum as the Cathode. *ACS Energy Lett.* **2017**, *2*, 1534–1538.

2. Zhou, G.; Zhao, Y.; Zu, C.; Manthiram, A. Free-Standing TiO_2 Nanowire-Embedded Graphene Hybrid Membrane for Advanced Li/Dissolved Polysulfide Batteries. *Nano Energy* **2015**, *12*, 240−249.